EXPERIMENTAL STUDY OF A DIAGONALLY REINFORCED BEAM WITH WELL REPAIRABILITY

Kazushi Shimazaki

Kanagawa University, Department of Architecture and Building Engineering,
Kanagawa-ku, Yokohama, 221-8686, JAPAN

ABSTRACT

Since the Great Hanshin Earthquake, the demands of people who own buildings have changed: they want to use the buildings again with small repair cost. This requires good repairability of RC members. A beam with diagonal reinforcements is very ductile, however, the diagonal reinforcements yield on the tension side only because concrete struts will work with them on the compression side. When the diagonal reinforcements yield under tension, tension stress is applied to the concrete along the whole length by bond stress. This increases the number of concrete cracks. The results of this experimental investigation demonstrated that unbonded diagonal reinforcements are an effective means to reduce damage to short beams and have the same energy dissipation ability as bonded ones. A small design at the end of the beam can make the diagonal reinforcements yield on the compression side, and not increase the beam length.

Keywords: RC structure, damage control, diagonally reinforced beam, earthquake resistance design

INTRODUCTION

The goal of the earthquake resistant design of any country is to protect life in very severe earthquakes by providing for buildings with strength and toughness to resist collapse. After big earthquakes such as the Great Hanshin Earthquake, however, the demands of people who own buildings have changed: they want to use the buildings again with small repair cost. This requires good repairability of RC members.

For reinforced concrete buildings with a "shear core", short beams are connected the shear walls as shown in Figure 1. To satisfy the ductility demand of the beams, diagonal reinforcements have been used [1]. Many experimental studies were carried out in Japan on using diagonal reinforced beams as members of a tube structure [e.g. 2,3]. Although these beams showed very ductile behavior, the number of concrete cracks was very large and damage to the beams prevented repair works. In those beams, the diagonal reinforcements yield on the tension side only because concrete struts work with them on the compression
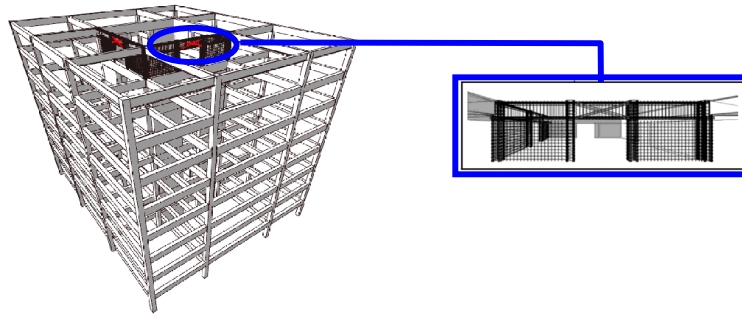
1

Figure 1: Short beams in a reinforced concrete buildings with shear core

side. This increases the number of concrete cracks, and increases the beam length. Repair works are thus laborious.

The working stress of diagonal reinforcements is constant with respect to the overall length, so there is no need for bond stress between the diagonal reinforcements and concrete. Unbonded diagonal reinforcements are one solution to reduce the number of concrete cracks. A small design at the end of the beam can make the diagonal reinforcements yield on the compression side. This means the ability to absorb energy will increase and the beam length will not increase.

This paper describes a study on short beams with diagonal reinforcements to reduce concrete cracks and thus improve repairability.

EXPERIMENTAL PROGRAM

Test specimens

The dimensions of the specimens are shown in Figure 2. All beams had eight diagonal reinforcement bars with four longitudinal reinforcement bars and web reinforcements. The section is 200 mm thick, 400 mm high, and 1000 mm long. The overall length of the specimen is 2800 mm with end stubs of 400 mm thickness, 1400 mm height and 900 mm length at both ends. These dimensions are one third scale of the prototype structure shown in Figure 1.
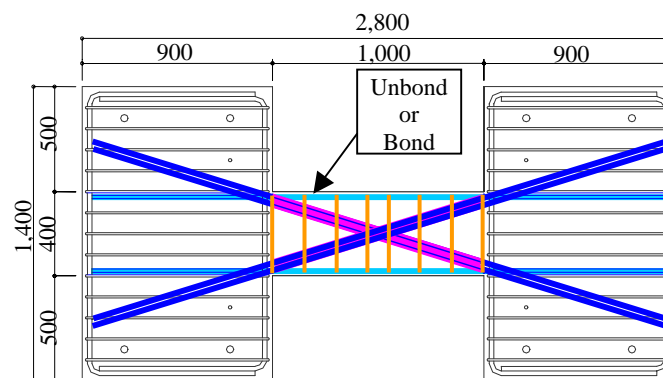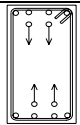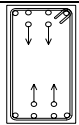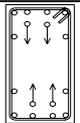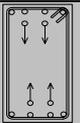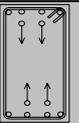

Figure 2: Dimensions of Test Specimens

The primary experimental parameter is the bond of diagonal reinforcements, and the second is the amount of web reinforcement as shown in Table 1. The diagonal and longitudinal reinforcements in the web are the same in four specimens (#1, #2, #4, #5). Specimens #1 and #4 are common diagonal reinforcement beams, and specimens #2 and #5 are beams with

unbonded diagonal reinforcements. Specimen #3 has a gap filled by rubber at the end of the beam to allow yield of the diagonal reinforcement at compression. Additional reinforcements (2D-16 at one quarter and three quarters of the section) are placed to cover for the deficit section. The amount of web reinforcement provided for #1, #2 and #3 is consistent with the current AIJ standard [4, experimental equation]. For #4 and #5, the amount is calculated according to the AIJ design guidelines [5, truss model equation] with R=1/50 inelastic rotational ability. In the design, the concrete compressive strength was assumed to be 48 N/mm^2 (σ_B=54 N/mm^2), the yield stress of the main reinforcement was assumed to be 390 N/mm^2 (σ_y=476 N/mm^2), and the yield stress of the web reinforcement was assumed to be 295 N/mm^2 (σ_y=372 N/mm^2). This paper examines specimens #1 to #3 mainly.

Table 1 : List of specimens

Specimen	No.1	No.2	No.3	No.4	No.5	No.6, , ,
Section						on going
b×D(mm)	200×400	200×400	200×400	200×400	200×400	
σ_B(N/mm^2)	54	54	54	54	54	
Parallel	2-D16	2-D16	4-D16	2-D16	2-D16	
X Shape	4-D16 Bond	4-D16 Un-bond	4-D16 Un-bond	4-D16 Bond	4-D16 Un-bond	
P_t(%)	1.51	1.51	2.01	1.51	1.51	
Web	2-D6 @150	2-D6 @150	2-D6 @150	2-D6 @100	2-D6 @100	
P_w(%)	0.21	0.21	0.21	0.32	0.32	

Unbonded reinforcement
To create unbonded reinforcement bars, wax and thin plastic sheets were used. First, dimple parts of a deformed bar were filled by wax, and then the bar was covered by a thin plastic sheet as shown in Figure 3. The anchor part (the part in a stub) was untouched.

(a) Step 1 : Wax coating   (b) Step 2 : Covered by a thin plastic sheet
Figure 3 : Unbonded reinforcement bar

Test setup
The bottom of the specimen rotated 90 degrees was bolted to the loading frame. A 500 mm wide by 600 mm deep L shaped loading beam was placed on top of the specimen, and a main
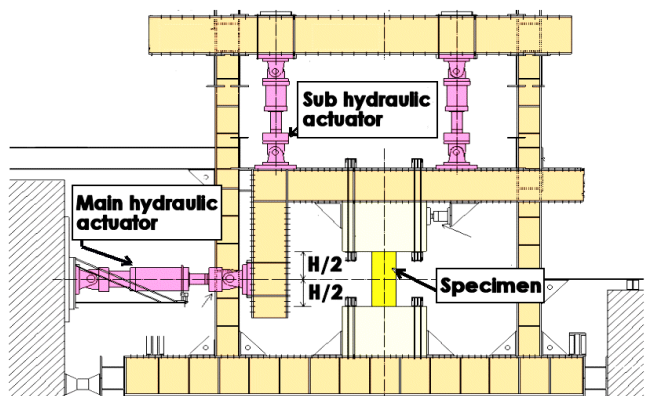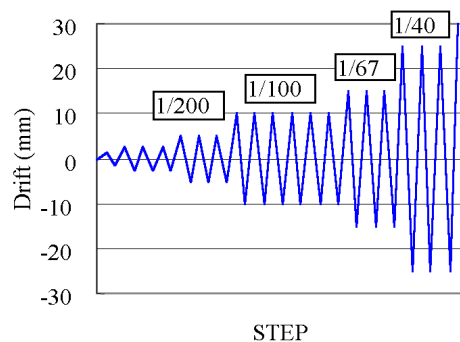

Figure 4 : Test Setup

Figure 5 : Loading Cycles

3

hydraulic actuator was attached at mid-height of the beam. Two sub hydraulic actuators were attached at the top to control the level of loading beam as shown in Figure 4. Antisymmetric bending moment was applied to the specimen.

Loading Cycles

Loading cycles as shown in Figure 5 were applied to increase the drift angle *R* with 3 repeated cycles. Only at the level of R=1/100, the loading cycle was conducted with 6 repeated cycles. These were determined by dynamic response analysis for the prototype building shown in Figure 1 during a severe earthquake to satisfy the energy dissipation ability.

Instrumentation

During the tests, total drift was measured as the displacement difference of the loading stubs. Partitioned axial displacements to calculate bending deformation were measured at both flanges as shown in Figure 6. Shear deformation was calculated by subtracting the calculated bending deformation from the measured total deformation. Strains of reinforcements were also measured by strain gauges mounted in several locations along diagonal reinforcements, longitudinal reinforcements and on the transverse bars.

Figure 6 : Measurement of partitioned axial displacements at both flanges

EXPERIMENTAL RESULTS

Crack patterns

During the response in the R=1/700 cycle, bending cracks were observed for all specimens at beam ends. In the R=1/400 cycle, bending-shear cracks were observed. For the specimens with bonded diagonal reinforcements (#1), diagonal shear cracks occurred at the center in the R=1/100 cycle. For the specimen with unbonded diagonal reinforcements (#2), cracks concentrated on both edge parts with no shear crack at the center and the number of cracks was small. Crack patterns in the R=1/100 and R=1/67 cycles are shown in Figures 7 and 8.
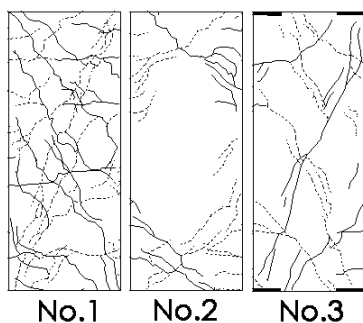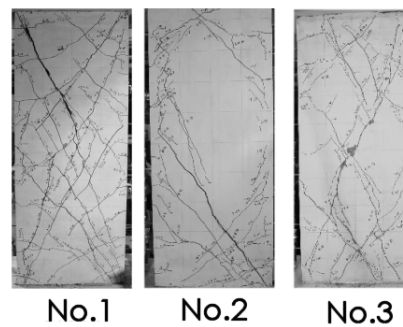

Figure 7 : Crack Patterns (R=1/100) **Figure 8 :** Crack Patterns (R=1/67)

Load-deflection curves

The load-deflection behaviors of the specimens are shown in Figure 9 for specimens #1, #2 and #3. Significant differences are not observed between the hysteretic response of the specimens until the R=1/40 cycle. During the response in the R=1/40 cycle, strength

degradation was observed because of shear yield for specimens #1 and #3, and of bond failure for specimen #2. As specimen #3 has gaps at both ends, the tangent stiffness in the R= 1/100 cycle is rather small. In contrast, the reaction force in the R=1/67 cycle is larger, because it has additional longitudinal reinforcements.
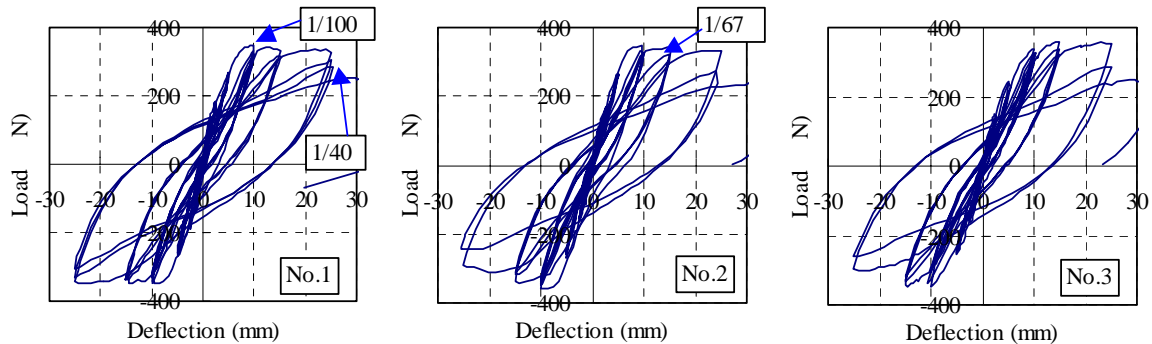

Figure 9 : Load-Deflection Curves

The force-displacement behavior can be predicted based on the assumption that the behavior is the sum of a parallel-reinforced R/C beam and diagonal steel braces. For the R/C beam, the flexural crack M_c and yield strength M_y are calculated by the approximate equations (1) and (2), and the stiffness reduction factor α_y (Secant modulus at yield point/Initial stiffness) is obtained by experimental equation (3) [4].

$$M_c=0.56\sqrt{\sigma_B}Z \qquad \text{(units: N, mm)} \tag{1}$$

$$M_y=0.9a_t\sigma_y d \tag{2}$$

$$\alpha_y=(-0.0836+0.159a/d)(d/D)^2 \tag{3}$$

where, σ_B is concrete strength in N/mm^2, Z is section modulus, a_t is area of longitudinal tension reinforcement, σ_y is yield strength of steel, d is distance from extreme compression fiber to centroid of tension reinforcement, D is height of beam, and a is the shear span length (M/Q). The diagonal reinforcements are assumed to be the bi-linear system and to act in both tension and compression.

The envelope curves of the test results are compared with the calculated load-deflection relations in Figure 10. Both show good agreement. This approximate calculation method can estimate the load-deflection behavior for diagonally reinforcement beams while fully satisfying the design.
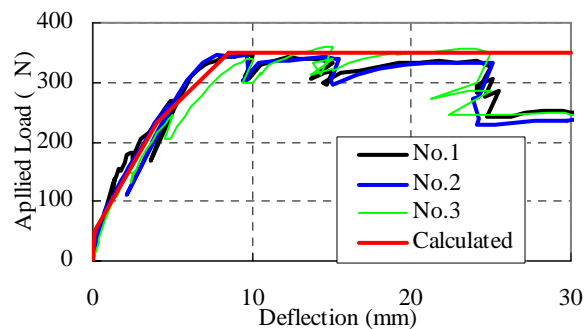

Figure 10 : Load-Deflection Curves

5

Strain of reinforcements

Figure 11 shows the strain distribution of the diagonal reinforcements at the first peak load in each cycle. Strains of the unbonded reinforcements (#2, #3) are almost uniform in each cycle even on the compression side, in contrast with the bonded one, in which the strain was influenced by bending moment on the compression side. The reinforcements yielded during cycle R=1/200 to R=1/100 for all specimens. The reinforcements of specimen #3 which has gaps at both ends of the beam, yielded on both the tension and compression sides. Compression strain of specimen #2 is small because the concrete struts act in compression.
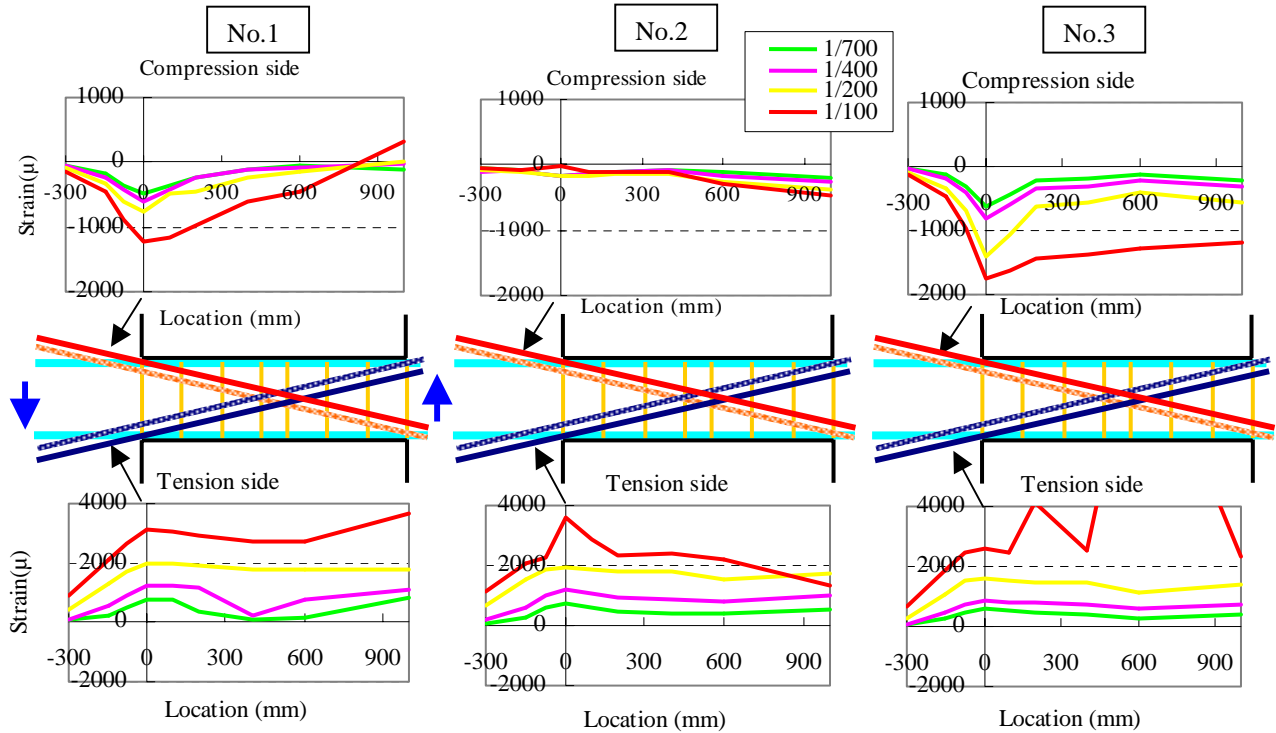
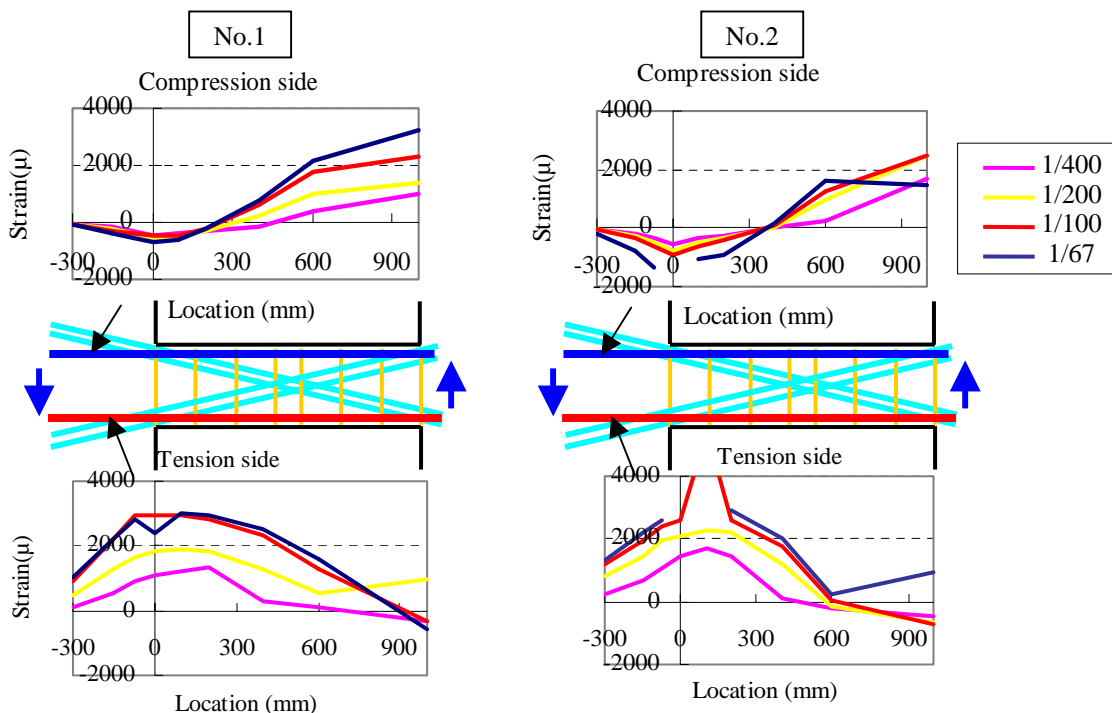**Figure 11 :** Strain distribution of diagonal reinforcements

Figure 12 : Strain distribution of parallel reinforcements

Figure 12 shows the strain distribution of the parallel reinforcements at the first peak load in each cycle for specimens #1 and #2. During cycle R=1/200 to R=1/100, the decline angle of strain distribution on the tension side is larger in specimen #2 than in #1. This is caused by the difference of compression strain of the diagonal reinforcements shown in Figure 11. This means the bond stress in specimen #2 is larger than in #1, and it is a severe value for bond failure.

Figure 13 shows the strain distribution of the web reinforcements at the first peak load in each cycle. Dotted lines on the right side in each figure are drown assuming symmetry, and were not measured. The web reinforcements yielded at the center of the beam in the R=1/100 cycle for specimen #1, in contrast with specimen #2 which yielded at the end of the beam in the R=1/67 cycle. Specimen #3 behaved intermediate between #1 and #2. These tendencies match the crack patterns shown in Figures 7 and 8.
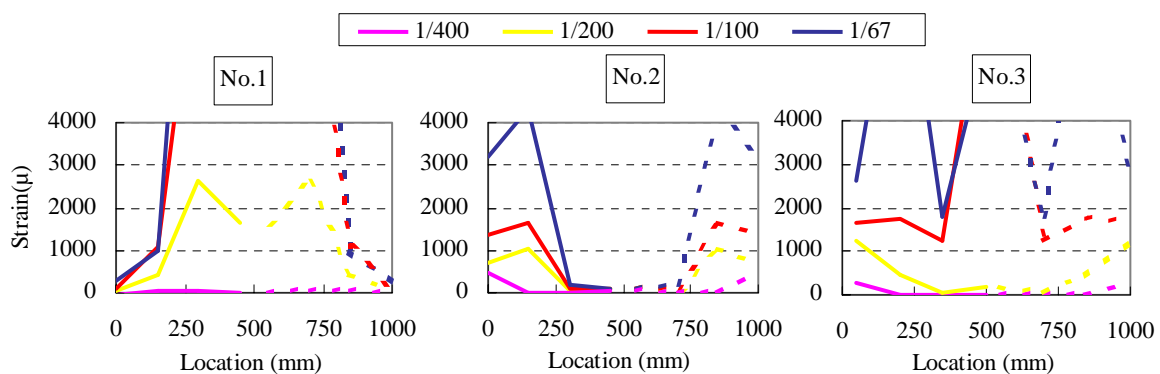

Figure 13 : Strain distribution of web reinforcements

Bending and shear deformation
Bending deformation was calculated by integrating the curvature obtained from the piecewise axial displacement difference of both flanges. Shear deformation was calculated by subtracting the bending deformation from the total deformation.

Figure 14 shows the change of deformation components of bending deformation and shear deformation. The shear deformation part increases with increasing total deformation caused by shear cracks. Specimen #1 had shear cracks in the center part, so the shear deformation part becomes much larger than that of specimen #2 which never cracked in the center. The shear cracks at the end part for specimen #2 caused a bending hinge at both beam-ends. For specimen #3, bending deformation was almost 100% in the elastic stage because the beam behaves like rocking deformation due to the gap at the end of the beam. After yielding of reinforcement bars, the deformation components of specimen #2 are between those of specimens #1 and #2.
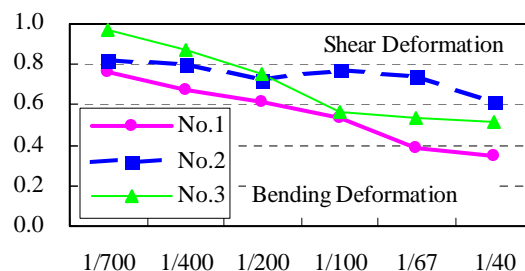

Figure 14 : Changing of deformation component

Axial elongation

Total axial elongation is calculated as the sum value of measured partitioned axial displacements. Figure 15 shows the relation between calculated axial elongation and drift deformation. Until the R=1/200 cycle, the accumulated axial elongation is not measured. At the R=1/100 cycle, the axial elongation increases for specimens #1 and #2 due to yielding of the diagonal and longitudinal reinforcements. The elongation is larger in specimen #2 than in specimen #1. This difference is caused by the compression strain of the diagonal reinforcements shown in Figure 11. The compression strain of bonded diagonal reinforcement becomes large, because the concrete is compressed by bending, and this compression stress is propagated to the diagonal bar by bond stress. The unbonded diagonal reinforcements are not influenced by the concrete compression stress, and act only as a compression brace. However, a concrete arch strut acts with them, so the compression stress of the unbonded diagonal reinforcements is small. As accumulated tension stress in the unbonded diagonal reinforcements became large, the axial elongation in specimen #2 became large. There is no accumulated axial elongation in specimen #3 as expected.
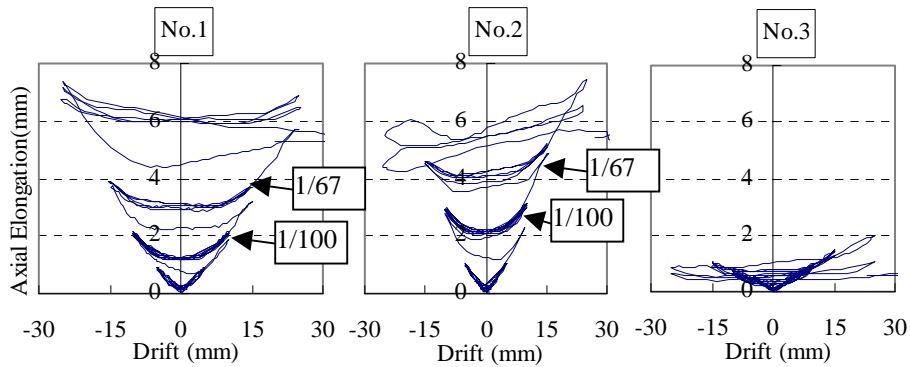

Figure 15 : Relation of axial elongation versus drift

Equivalent damping factor

Figure 16 shows the equivalent damping factor of each specimen calculated from the first half cycle of the applied load – total deflection relationship shown in Figure 9. Significant differences are not observed in the equivalent damping factor between specimens #1 and #2. The equivalent damping factor of specimen #3 is smaller than that of others in the first cycle because of stiffness reduction caused by the gaps at the critical section of the beam. In subsequent cycles, the values are close to others. This means that the energy dissipation ability is the same, despite the clear difference of crack patterns shown in Figures 7 and 8.
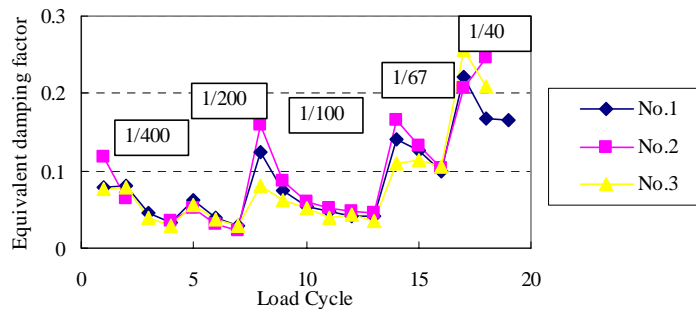

Figure 16 : Fluctuations in equivalent damping factor

CONCLUSIONS

This paper examined the behavior of short beams with diagonal reinforcements to reduce damage during a severe earthquake for good repairability. The main findings are follows:

1. The results of this experimental investigation demonstrated that unbonded diagonal reinforcements are an effective means to reduce the number of cracks for short beams.
2. Significant differences are not observed between the hysteretic response and equivalent damping factor of the specimens. The approximate calculation method (sum of a parallel reinforced R/C beam and diagonal steel braces) can estimate the load-deflection behavior for diagonally reinforcement beams while fully satisfying the design.
3. Strains of the unbonded diagonal reinforcements are almost uniform in each cycle and free from bending stress.
4. The web reinforcements yielded at the center of the beam for specimen #1, in contrast with specimen #2 which yielded at the end of the beam.
5. The axial elongation is larger in specimen #2 than in specimen #1. A small design at the end of the beam prevents elongation.

This report showed the results of a preliminary study. The project is continuing, and the effectiveness of web reinforcement and more detailed design for compression yield of diagonal reinforcements will be presented in the near future. Furthermore, despite the good agreement of the load-deflection behavior between the tests and the approximate calculation, the strain distribution in the reinforcements was different. This result suggests the possibility of a difference of the load resistance system between bonded and unbonded diagonally reinforced beams. These will be studied by analytical investigations.

REFERENCES

1. Park, R. and T. Paulay, Reinforced Concrete Structures, A WILEY-INTERSCIENCE PUBLICATION, 1975
2. Eto, H., K. Yoshioka, et al., Aseismic design of 41 story reinforced concrete tube structure –Part 4 Ultimate shear strength of short beams-, Summaries of technical papers of annual meeting, C, Architectural Institute of Japan, 1989, pp.773-774 (In Japanese)
3. Shimazaki, K. and Y. Hayakawa, Experimental study for ductility of short beams, Proceedings of the Japan Concrete Institute, 1990, pp.179-184 (In Japanese)
4. AIJ, AIJ Standard for structural Calculation of Reinforced concrete Structures –Based on Allowable Stress Concept–, Architectural Institute of Japan, 1999.
5. AIJ, Design Guidelines for Earthquake Resistant Reinforced Concrete Buildings Based on Inelastic Displacement Concept, Architectural Institute of Japan, 1999.